Electronic Supplementary Material (ESI) for Catalysis Science & Technology.

Supporting Information

A Doping Element Improving the Properties of Catalysis: In Situ Raman Spectroscopy Insight into Mn-doped NiMn Layered Double Hydroxide for Urea Oxidation Reaction

Xu Yang [1], Huimin Zhang [2], Wei Xu [1], Binbin Yu [3], Yan Liu [4], Zucheng Wu [1,*]

[1] Department of Environmental Engineering, Zhejiang University, Hangzhou 310058, China

[2] School of Civil Engineering and Architecture, East China Jiaotong University, Nanchang 330013, China

[3] College of Pharmaceutical and Materials Engineering, Taizhou University, Taizhou 318000, China

[4] School of Earth Sciences, Zhejiang University, Hangzhou 310027, China

*E-mail: wuzc@zju.edu.cn

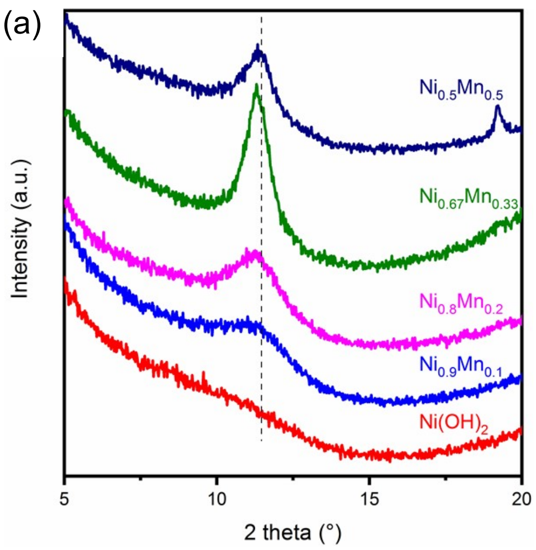
(a)
Intensity (a.u.)
2 theta (°)
5
10
15
20
Ni0.5Mn0.5
Ni0.67Mn0.33
Ni0.8Mn0.2
Ni0.9Mn0.1
Ni(OH)2

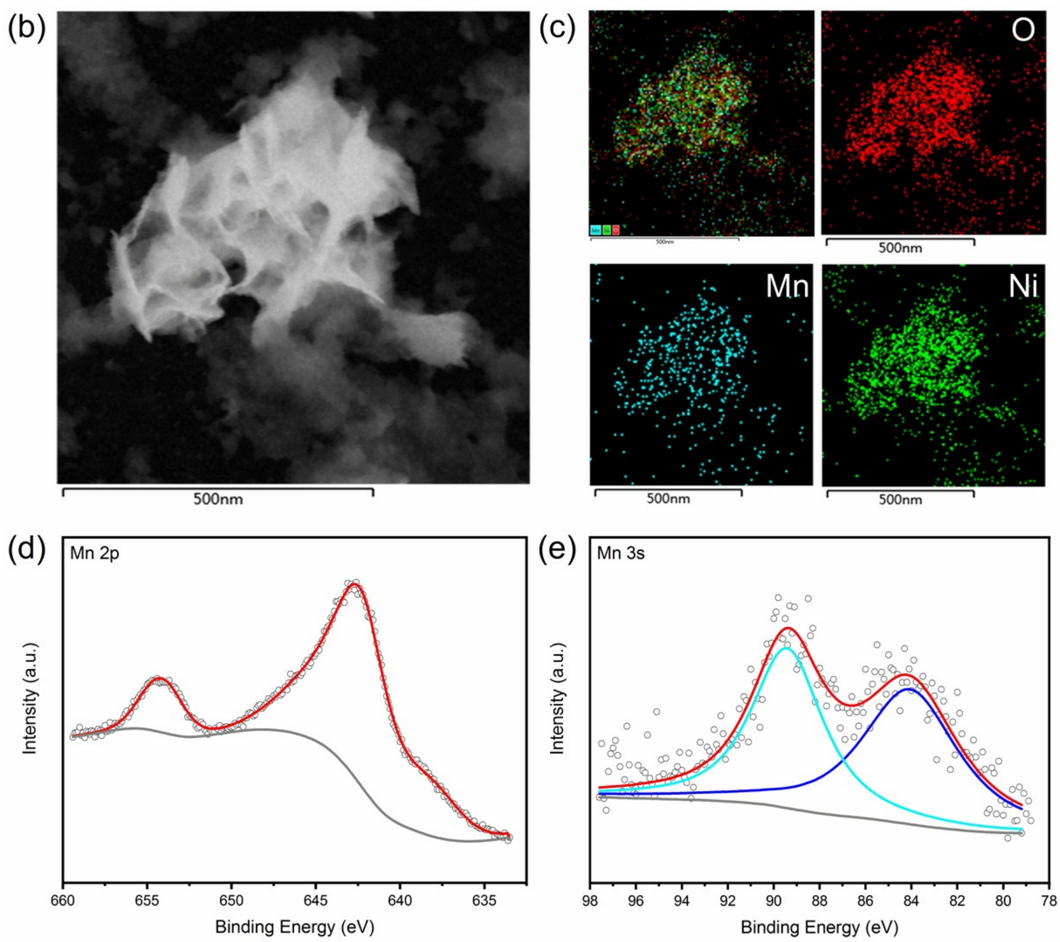
(b)
500nm
(c)
O
Mn
Ni
500nm
500nm
500nm
(d)
Mn 2p
Intensity (a.u.)
Binding Energy (eV)
660
655
650
645
640
635
(e)
Mn 3s
Intensity (a.u.)
Binding Energy (eV)
98
96
94
92
90
88
86
84
82
80
78

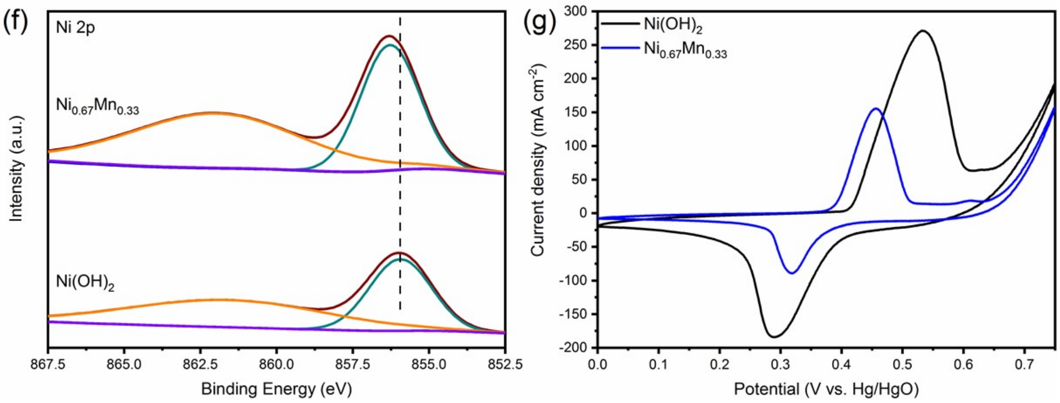

Figure S1. (a) Partially enlarged XRD patterns; (b) STEM image of $Ni_{0.67}Mn_{0.33}$ LDHs and (c) corresponding elemental mapping images of Ni, Mn and O; XPS spectra of (d) Mn 2p and (e) Mn 3s of $Ni_{0.67}Mn_{0.33}$/CFP; (f) XPS spectra of Ni $2p_{3/2}$ of the samples; (g) CV plots of the samples in 1 M KOH at 10 mV s^{-1}.

Note:

The scanning TEM (STEM) elemental mapping images were taken with a JEM-2100F microscope.

The heteroatom doping tends to cause the XPS Ni $2p_{3/2}$ peak position of the host $Ni(OH)_2$-based species to shift to the direction of high binding energy, which indicates a strong electronic interaction between the doping element and the host element, similar with those reported in literature.[1-4] In the CV of Mn-doped $Ni(OH)_2$, the lower oxidation peak potential and negatively shifted onset potential of Ni^{2+} oxidation also reflect this electronic interaction implying a higher oxidation state. The consistence of both CV and XPS showed a higher oxidation capacity of the Ni species doped with Mn.

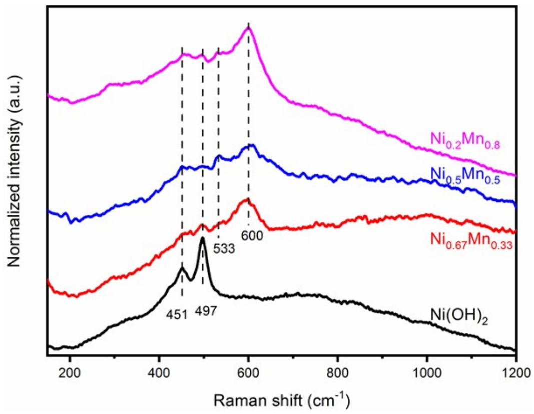

Figure S2. Raman spectra for NiMn samples under open circuit potential conditions in 1 M KOH.

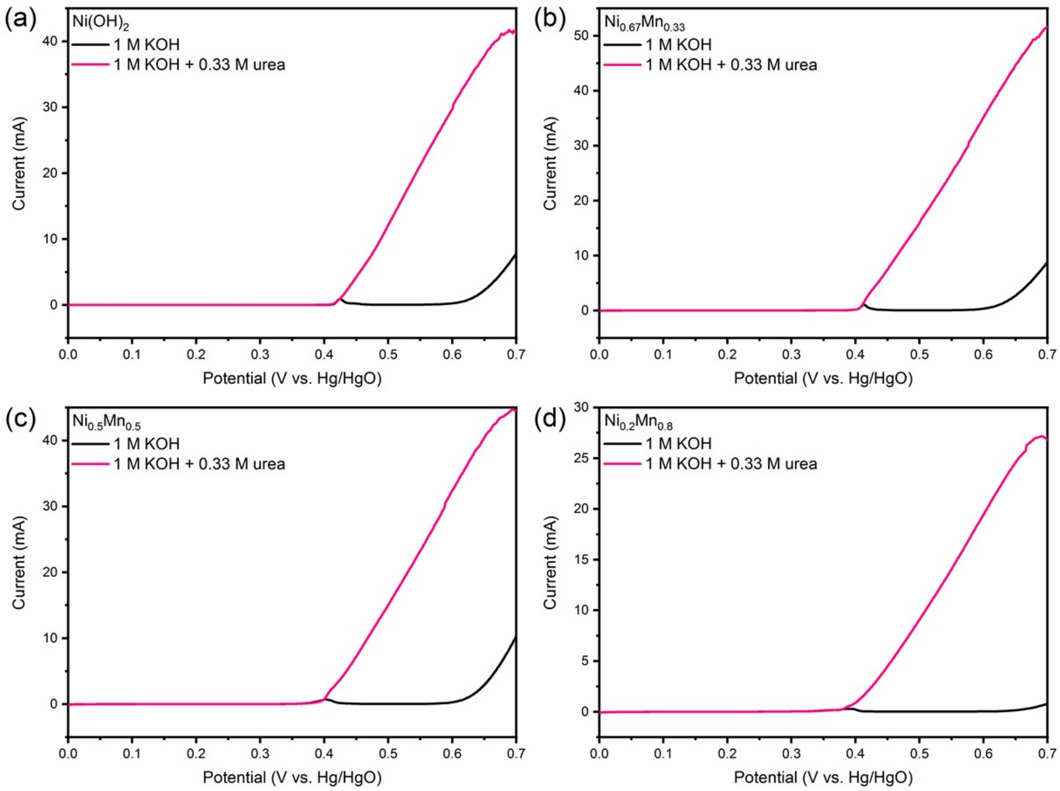

Figure S3. (a−d) LSV curves of Au foil supported $Ni(OH)_2$ and NiMn with desired metal ratios in 1 M KOH and 1 M KOH + 0.33 M urea at a scan rate of 1 mV s^{-1}.

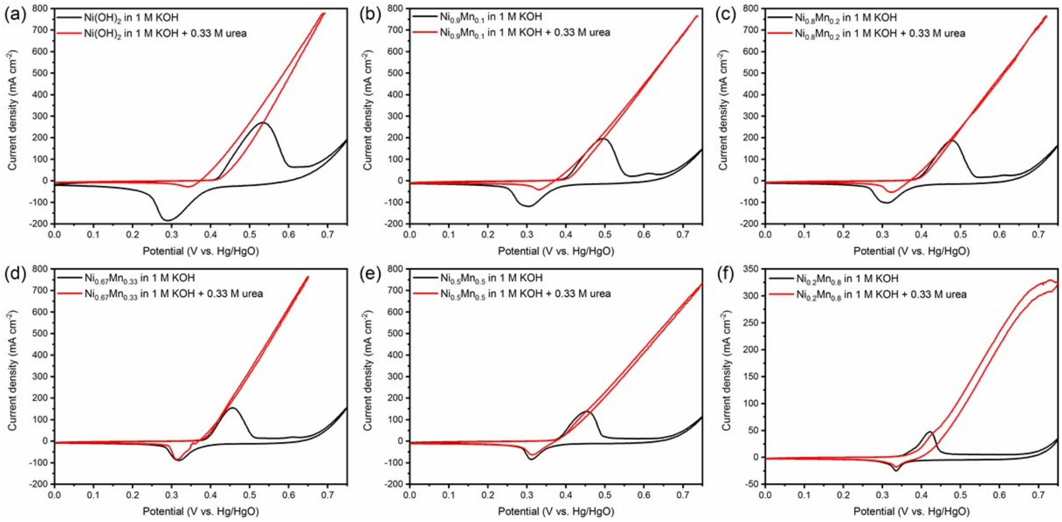

Figure S4. CV curves of (a) $Ni(OH)_2$/CFP and (b−f) $Ni_{1-x}Mn_x$/CFP in 1 M KOH and 1 M KOH + 0.33 M urea at a scan rate of 10 mV s^{-1}.

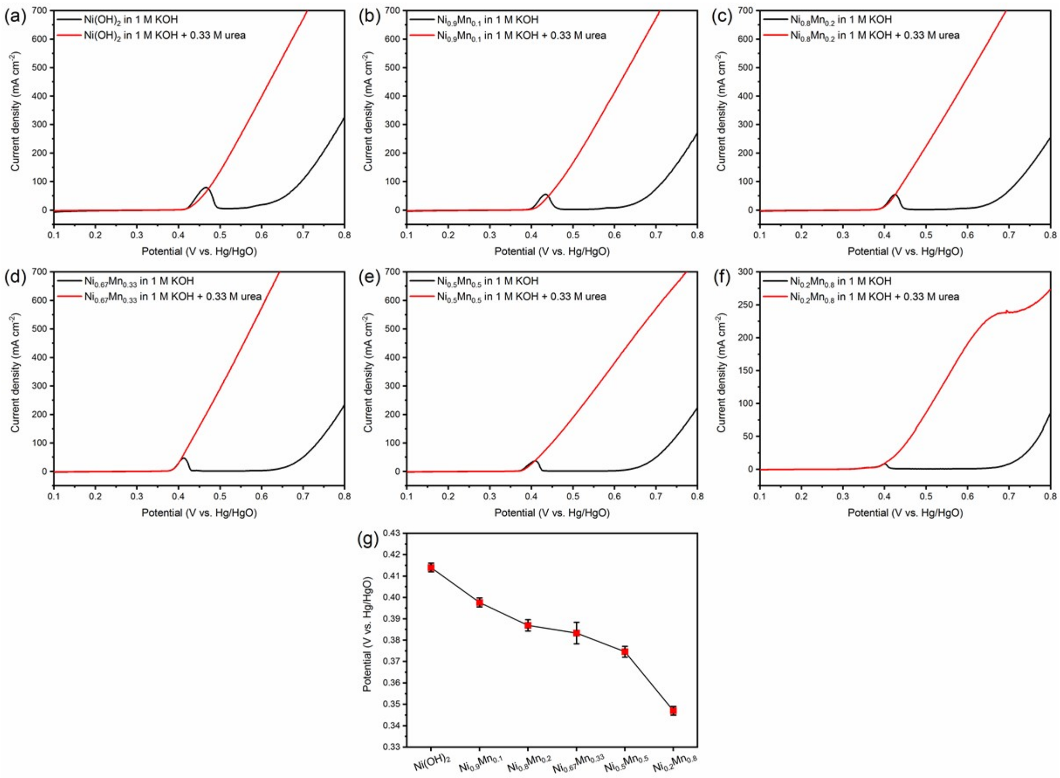

Figure S5. (a−f) LSV curves of $Ni(OH)_2$/CFP and $Ni_{1-x}Mn_x$/CFP in 1 M KOH and 1 M KOH + 0.33 M urea at a scan rate of 1 mV s^{-1}; (g) UOR onset potentials of the samples with various Mn content in 1 M KOH + 0.33 M urea. Error bars indicate the standard deviation of three tests.

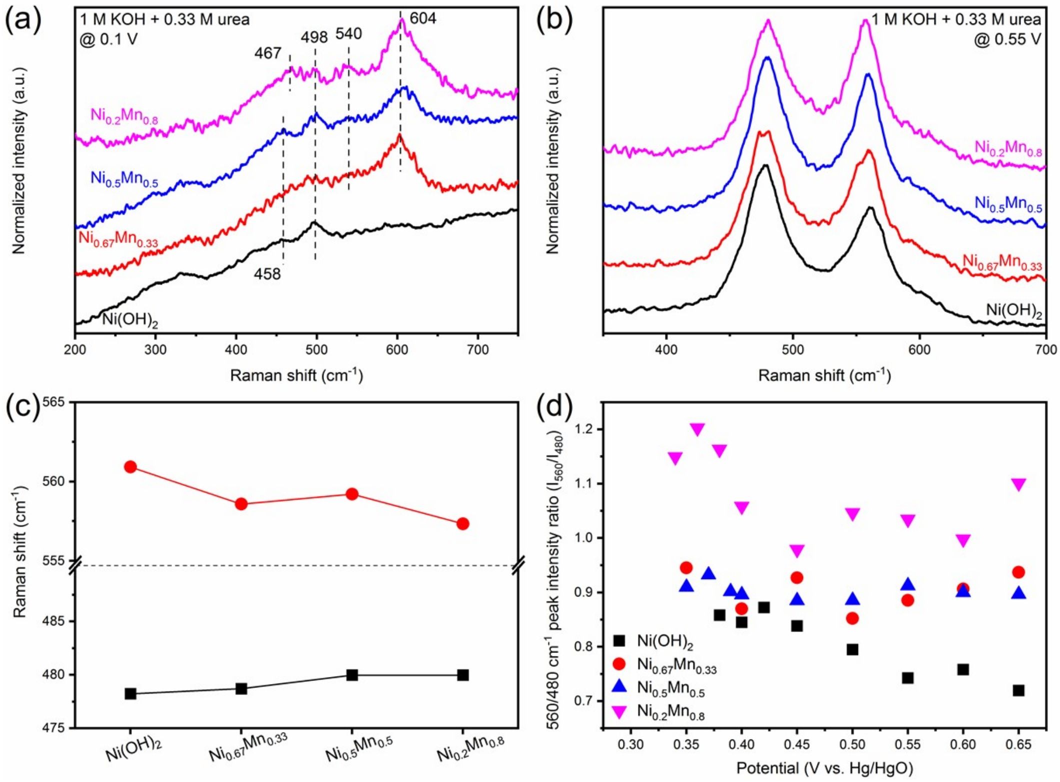

Figure S6. (a−b) In situ Raman spectra of the four samples at 0.1 V and 0.55 V vs. Hg/HgO; (c) Raman peak positions of the two main bands corresponding to Ni−O in NiOOH of the four samples at 0.55 V; (d) the 560 cm^{-1}/480 cm^{-1} Raman peak intensity ratio (I_{560}/I_{480}) versus the applied potential. Electrolyte condition: 1 M KOH + 0.33 M urea.

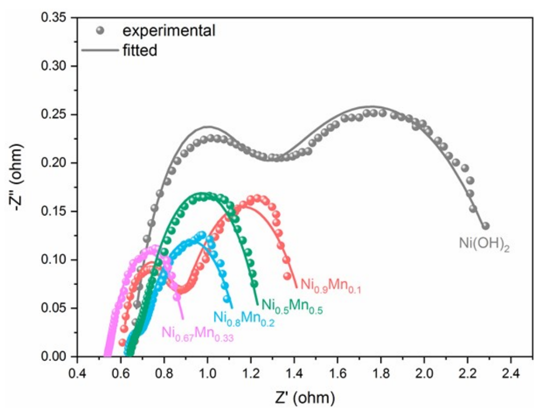

Figure S7. Nyquist plots collected for the samples in 1 M KOH + 0.33 M urea at 0.45 V vs. Hg/HgO.

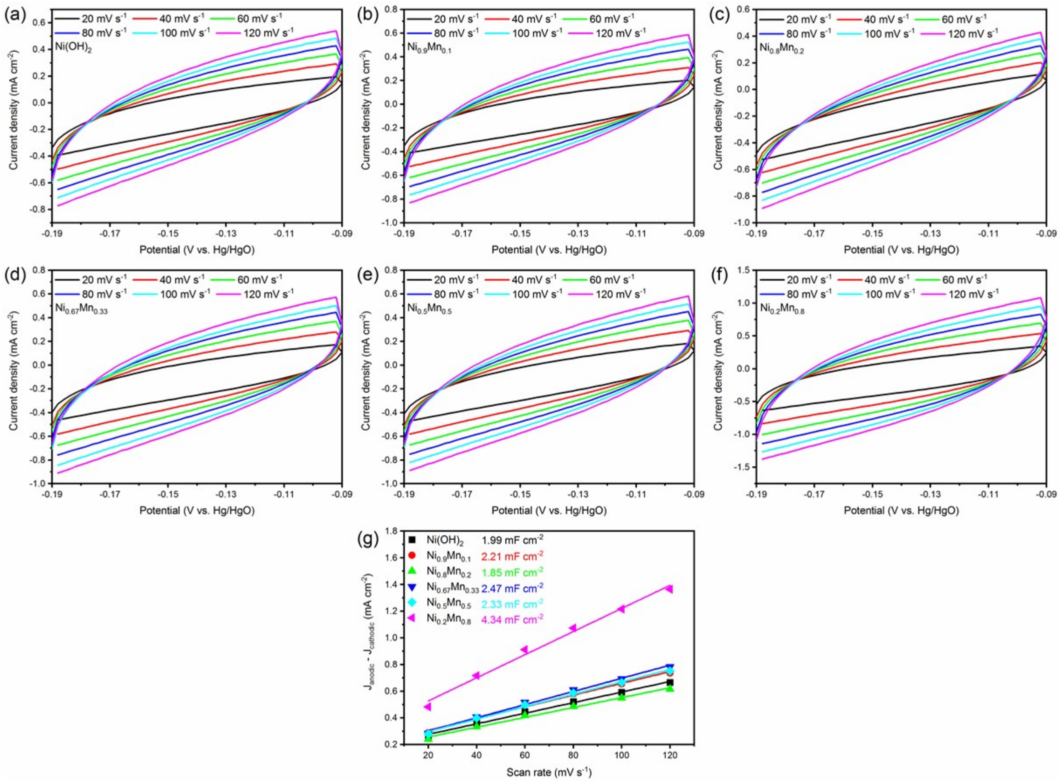

Figure S8. (a−f) CV curves of $Ni(OH)_2$/CFP, $Ni_{1-x}Mn_x$/CFP samples in a narrow potential range for non-Faraday reaction in 1 M KOH with different scan rates; (g) estimation of electrochemical double layer capacitance (C_{dl}) of the samples.

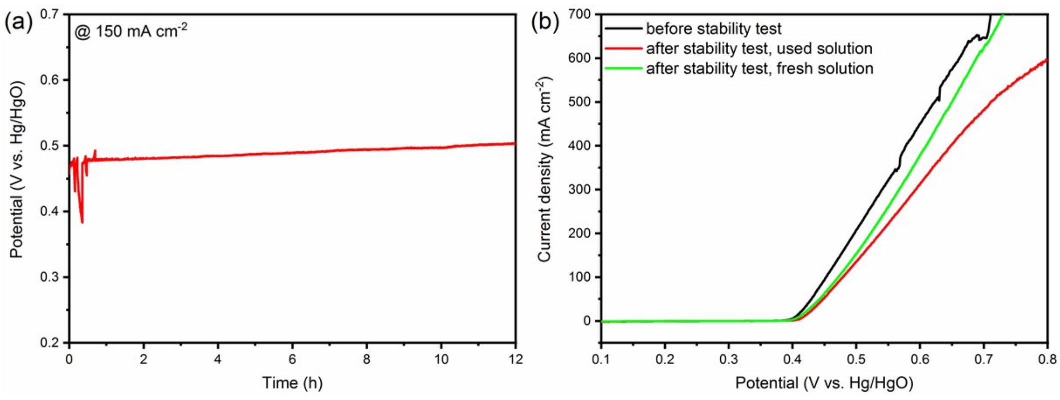

Figure S9. (a) The long-term stability performance of $Ni_{0.67}Mn_{0.33}$/CFP at a constant current density of 150 mA cm^{-2}; (b) comparison of LSV plots of $Ni_{0.67}Mn_{0.33}$/CFP before and after stability test. The electrolyte: 1 M KOH + 0.33 M urea. The LSV scan rate: 1 mV s^{-1}.

Table S1. The catalyst loadings of $Ni(OH)_2$/CFP and $Ni_{1-x}Mn_x$/CFP samples, and elemental compositions for $Ni_{1-x}Mn_x$/CFP samples.

Sample	**Catalyst loading (mg cm^{-2})**	**Ni:Mn atomic ratio**
$Ni(OH)_2$/CFP	2.48	-
$Ni_{0.9}Mn_{0.1}$/CFP	2.74	0.93:0.07
$Ni_{0.8}Mn_{0.2}$/CFP	2.64	0.84:0.16
$Ni_{0.67}Mn_{0.33}$/CFP	2.55	0.68:0.32
$Ni_{0.5}Mn_{0.5}$/CFP	2.90	0.55:0.45
$Ni_{0.2}Mn_{0.8}$/CFP	2.50	0.18:0.82

Table S2. Comparison of the electrocatalytic UOR performance of recent NiMn compound catalysts.

Sample	Electrolyte	Performance	Stability	Reference
$Ni_{0.67}Mn_{0.33}$ LDH/CFP	1 M KOH + 0.33 M urea	510.8 mA cm^{-2} @ 0.6 V vs. Hg/HgO [a)]	12 h @ 150 mA cm^{-2}	This work
Mn-doped $Ni(OH)_2$/CP	1 M KOH + 0.5 M urea	133.7 mA cm^{-2} @ 1.45 V vs. RHE [b)]	42 h @ 1.385 V vs. RHE below 55 mA cm^{-2} in 1 M KOH with continued refreshing of 0.5 M urea	ACS EST Engg., 2022, DOI: 10.1021/acsestengg.1c00400.
Ni foam@Ni-MnO_2	1 M KOH + 0.33 M urea	150 mA cm^{-2} @ 0.60 V vs. SCE [c)]	5 h @ 0.5 V vs. SCE	J. Alloys Compd., 2022, 894, 162515
Ultrathin NiMn-LDH/CFC	1 M KOH + 0.5 M urea	20 mA cm^{-2} @ 1.351 V vs. RHE [b)]	25 h @ ≈34 mA cm^{-2}, reduction of 2.8%	Appl. Catal. A: Gen., 2021, 614, 118049
Striped (Mn,Ni)O(OH)/NF	1 M KOH + 0.5 M urea	100 mA cm^{-2} @ 1.40 V vs. RHE [b)]	10 h @ 10 mA cm^{-2}	Surf. Coat. Technol., 2021, 408, 126799
Mn-Ni_3S_2/NF-0.2	1 M KOH + 0.5 M urea	100 mA cm^{-2} @ 1.397 V vs. RHE [c)]	20000 s @ 1.424 V vs. RHE	ACS Sustainable Chem. Eng., 2020, 8, 8348−8355
NiMn-CNFs 10%	1 M KOH + 2 M urea	Peak current density of 79 mA cm^{-2} (at 50 mV s^{-1}) [c)]	Multistep chronoamperometry from 0.4 to 1.2 V vs. RHE within 2700 s	Int. J. Hydrogen Energy, 2018, 43, 5561−5575
Mn-$Ni(OH)_2$/CFC	1 M KOH + 0.5 M urea	100 mA cm^{-2} @ ≈1.52 V vs. RHE [a)]	11 h @ ≈20 mA cm^{-2}	Chem. Commun., 2017, 53, 10711
NiMn-CNFs	1 M KOH + 1 M urea	Peak current density of 300	900 s @ 0.6 V vs. Ag/AgCl in 1 M	Appl. Catal. A: Gen., 2016, 510, 180–188

		mA cm^{-2} g^{-1} (at 50 mV s^{-1}) [c)]	KOH + 2 M urea, from ≈350 mA cm^{-2} g^{-1} to ≈150 mA cm^{-2} g^{-1}	
$Ni_{1.5}Mn_{1.5}O_4$/C	1 M KOH + 0.33 M urea	Peak current density of 6.9 mA cm^{-2} (at 10 mV s^{-1}, 50 μg cm^{-2}) [c)]	1000 s @ 0.5 V vs. Ag/AgCl	ACS Appl. Mater. Interfaces, 2016, 8, 12176−12185
Ni–Mn–Se/NF	1 M KOH + 0.33 M urea	400 mA cm^{-2} @ ≈1.53 V vs. RHE [b)]	50 h @ 200 mA cm^{-2}, from 1.474 V to 1.492 V (vs. RHE)	Chem. Commun., 2022, 58, 3545–3548
N-$Ni_1Co_3Mn_{0.4}O$/NF	1 M KOH + 0.5 M urea	100 mA cm^{-2} @ 1.399 V vs. RHE [c)]	2000 CV cycles	Int. J. Hydrogen Energy, 2022, 47, 5766–5778

Note: a) without iR correction; b) with iR correction; c) unknown whether iR correction was used.

CFP: carbon fiber paper; CP: carbon paper; CFC: carbon fiber cloth; CNF: carbon nanofiber; NF: Ni foam.

References:

[1] X. H. Sun, Q. Shao, Y. C. Pi, J. Guo and X. Q. Huang, *J. Mater. Chem. A*, 2017, 5, 7769-7775.

[2] X. Zhang, G. Liu, C. Zhao, G. Wang, Y. Zhang, H. Zhang and H. Zhao, *Chem. Commun.*, 2017, 53, 10711-10714.

[3] B. Dong, W. Li, X. X. Huang, Z. S. Ali, T. Zhang, Z. Y. Yang and Y. L. Hou, *Nano Energy*, 2019, 55, 37-41.

[4] Y. P. Lin, H. Wang, C. K. Peng, L. M. Bu, C. L. Chiang, K. Tian, Y. Zhao, J. Q. Zhao, Y. G. Lin, J. M. Lee and L. J. Gao, *Small*, 2020, 16, 2002426.